

# SPARSE: Scattering Poles and Amplitudes from Radial Schrödinger Equations

Roberto Bruschini\*

Department of Physics, The Ohio State University  
Columbus, Ohio 43210, USA

November 27, 2025

*GitHub repository link:* [github.com/Robrusch/SPARSE](https://github.com/Robrusch/SPARSE)

## Abstract

We introduce an algorithm for the solution of a large system of radial Schrödinger equations for scattering states. The system of differential equations is approximated as an ordinary linear nonhomogeneous system using the finite difference method. Dirichlet boundary conditions are imposed at the origin and at an arbitrary large radius. The  $K$ -matrix for physical energies is calculated from the numerical solutions of the system by comparison to the analytical real solutions at large distances. Scattering poles and amplitudes are calculated from the physical  $K$ -matrix.

---

\*[roberto.bruschini@tum.de](mailto:roberto.bruschini@tum.de)

# 1 Introduction

The Schrödinger equation applies to scattering states just as well as to bound states. In fact, the Schrödinger equation provides the foundation of many approximate analytical methods to calculate scattering poles and amplitudes using nonrelativistic quantum mechanics. But the advantages of calculating scattering poles and amplitudes directly from the Schrödinger equation are often overlooked.

The most obvious benefit of calculating scattering states directly from the Schrödinger equation is that it does not require any secondary approximation that may deteriorate the accuracy of the results. The scattering wavefunctions are completely determined by the Schrödinger equation, which in turn is completely determined by the potential and the masses of the degrees of freedom. Therefore, the scattering poles and amplitudes obtained in this way are just as good as the model or framework in which the Schrödinger equation is defined. That is most advantageous for those cases where resonant line shapes overlap with one another or with the energy thresholds where scattering channels open up. There is no need for a special treatment of esoteric structures like dips and cusps in the scattering amplitudes, since they are automatically included in the Schrödinger equation.

A system of Schrödinger equations can be used to describe the quantum mechanical scattering of particles in systems where different final states are possible after a collision at nonrelativistic center-of-mass energies. One notable example is nucleon-nucleon scattering, where inelastic effects start to play a role at relatively low scattering momenta ( $NN \rightarrow NN, N\Delta, NN', \Delta\Delta, \dots$ ).

In this paper, we introduce a simple yet effective algorithm for calculating scattering poles and amplitudes directly from a system of radial Schrödinger equations. Our method is to solve the system using a simple finite-difference method (see Chapter 3 of Reference [1]). Other common methods include propagation algorithms [2, 3] or basis expansions [4, 5] (see Reference [1] for a review). The crudeness of the finite-difference method is offset by its efficiency, which makes it the gold standard for numerically solving a differential equation with minimal effort.

In phenomenological applications, there are many situations in which one has to solve a system of Schrödinger equations several times to obtain a definite prediction. For instance, one may need to fit the parameters of some potential model, or one may want to estimate the error on the calculated spectrum from the uncertainty of the potential parameters using a bootstrap method. In those cases, it is desirable to have an algorithm that solves the system of Schrödinger equations as efficiently as possible. The extreme efficiency of the finite-difference method allows to solve systems with tens of coupled Schrödinger equations<sup>1</sup> using only modest computing power and time. That is the main purpose and novelty of the SPARSE algorithm.

The rest of the paper is structured as follows. In Section 2, we derive the system of radial Schrödinger equations describing an inelastic two-body scattering process in a partial wave with definite total-angular-momentum quantum numbers. In Section 3, we reduce the system of radial Schrödinger equations down to a nonhomogeneous linear system. In Section 4, we calculate the reactance matrix  $K$  for the scattering process by comparing the numerical wavefunctions to the analytic ones for scattering states with real boundary conditions. In Section 5, we review the calculation of scattering poles and amplitudes from the  $K$ -matrix. In Section 6, we showcase the SPARSE algorithm using a simple example that serves also as a tutorial. Finally, we summarize these results in Section 7.

## 2 Radial Schrödinger equation

A two-body elastic or inelastic scattering process at nonrelativistic energies can be described by a system of coupled Schrödinger equations. Using matrix notation, the system can be written concisely as

$$\left[ \frac{p_1^2}{2m_1} + \frac{p_2^2}{2m_2} + V(\mathbf{r}_1 - \mathbf{r}_2) - E \right] \psi(\mathbf{r}_1, \mathbf{r}_2) = 0, \quad (1)$$

---

<sup>1</sup>Such as the equations governing certain strongly interacting systems in the Born-Oppenheimer approximation for quantum chromodynamics; see, for instance, Ref. [6].

where  $\mathbf{r}_1, \mathbf{r}_2$  are the particles' coordinates,  $\mathbf{p}_1 = -i\nabla_{\mathbf{r}_1}, \mathbf{p}_2 = -i\nabla_{\mathbf{r}_2}$  are their conjugate momenta,  $m_1$  and  $m_2$  are diagonal mass matrices,  $V(\mathbf{r}_1 - \mathbf{r}_2)$  is a spin-dependent potential matrix,  $E$  is the total energy, and  $\psi(\mathbf{r}_1, \mathbf{r}_2)$  is a vector wavefunction. Note that we use natural units,  $\hbar = c = 1$ . Each Schrödinger equation in the system governs an elastic scattering process in a given channel. Each diagonal element of the mass matrices  $m_1$  and  $m_2$  contains the mass of the particles 1 and 2 in the corresponding channel. The couplings between the different Schrödinger equations introduce inelastic effects. In general, Equation (1) describes interacting particles with spin. Each component of the vector wavefunction  $\psi(\mathbf{r}_1, \mathbf{r}_2)$  contains the spin states of the scattering particles in the corresponding channel. Each element of the potential matrix  $V(\mathbf{r}_1 - \mathbf{r}_2)$  is an operator acting on the spin states.

We wish to reduce Equation (1) down to a system of differential equations in a single vector variable. Let us introduce the relative position

$$\mathbf{r} = \mathbf{r}_1 - \mathbf{r}_2 \quad (2)$$

and the center-of-average-mass position

$$\mathbf{R} = \frac{\bar{m}_1 \mathbf{r}_1 + \bar{m}_2 \mathbf{r}_2}{\bar{m}_1 + \bar{m}_2}, \quad (3)$$

where  $\bar{m}_1$  and  $\bar{m}_2$  are the average of the masses in the diagonal matrices  $m_1$  and  $m_2$ . We also introduce the relative momentum

$$\mathbf{p} = \frac{\bar{m}_2 \mathbf{p}_1 - \bar{m}_1 \mathbf{p}_2}{\bar{m}_1 + \bar{m}_2} \quad (4)$$

and the total momentum

$$\mathbf{P} = \mathbf{p}_1 + \mathbf{p}_2, \quad (5)$$

which are the momenta conjugate to  $\mathbf{r}$  and  $\mathbf{R}$ , that is,  $\mathbf{p} = -i\nabla_{\mathbf{r}}$  and  $\mathbf{P} = -i\nabla_{\mathbf{R}}$ . Expressing  $\mathbf{r}_1, \mathbf{r}_2, \mathbf{p}_1,$  and  $\mathbf{p}_2$  inside Equation (1) in terms of  $\mathbf{r},$

$\mathbf{R}$ ,  $\mathbf{p}$ , and  $\mathbf{P}$  using Equations (2)-(5), we obtain

$$\left[ \frac{p^2}{2\mu} + \left( \frac{\bar{m}_1}{m_1} - \frac{\bar{m}_2}{m_2} \right) \frac{\mathbf{p} \cdot \mathbf{P}}{\bar{m}_1 + \bar{m}_2} + \left( \frac{\bar{m}_1^2}{m_1} + \frac{\bar{m}_2^2}{m_2} \right) \frac{P^2}{2(\bar{m}_1 + \bar{m}_2)^2} + V(\mathbf{r}) - E \right] \psi(\mathbf{r}, \mathbf{R}) = 0, \quad (6)$$

where

$$\mu = \frac{m_1 m_2}{m_1 + m_2} \quad (7)$$

is a diagonal reduced-mass matrix. The system of Schrödinger equations is separable if the matrix multiplying  $\mathbf{p} \cdot \mathbf{P}$  is zero, which requires

$$\frac{\bar{m}_1}{m_1} = \frac{\bar{m}_2}{m_2}. \quad (8)$$

In this case, Equation (6) becomes

$$\left[ \frac{p^2}{2\mu} + \frac{P^2}{2(m_1 + m_2)} + V(\mathbf{r}) - E \right] \psi(\mathbf{r}, \mathbf{R}) = 0. \quad (9)$$

Then, separating  $\mathbf{R}$  and its conjugate momentum  $\mathbf{P}$  from Equation (9) produces a differential equation in the single vector variable  $\mathbf{r}$ ,

$$\left[ \frac{p^2}{2\mu} + V(\mathbf{r}) - E \right] \psi(\mathbf{r}) = 0, \quad (10)$$

where  $E$  now represents the energy in the center-of-momentum frame where  $\mathbf{P} = 0$ . Note that the separability condition in Equation (8) is satisfied exactly if and only if the two mass matrices are linearly dependent,  $m_1 \propto m_2$ . If  $m_1$  and  $m_2$  are linearly independent, Equation (8) cannot be satisfied exactly but Equation (6) may be approximately separable if

$$\left\| \frac{\bar{m}_1}{m_1} - \frac{\bar{m}_2}{m_2} \right\| \ll 1, \quad (11)$$

where the double vertical lines denote the matrix norm.

We now wish to further reduce Equation (10) to a system of differential

equations in the distance  $r = |\mathbf{r}|$ . Let us label the different Schrödinger equations in the system by an integer  $a$ . The Schrödinger equation in channel  $a$  reads

$$\sum_b \left[ \delta_{ab} \frac{p^2}{2\mu_a} + V_{ab}(\mathbf{r}) - \delta_{ab} E \right] \psi_b(\mathbf{r}) = 0, \quad (12)$$

where  $\psi_a(\mathbf{r})$  is the wavefunction in channel  $a$  and  $V_{ab}(\mathbf{r})$  are potential matrix elements. Recall that  $\psi_a(\mathbf{r})$  contains the spin states of the scattering particles and  $V_{ab}(\mathbf{r})$  is an operator acting on the spin states. Let  $J_{1,a}$  and  $J_{2,a}$  be the spins of the particles 1 and 2 in the channel  $a$ . We can expand the wavefunction  $\psi_a(\mathbf{r})$  as

$$\psi_a(\mathbf{r}) = \sum_{s,l} \sum_{\sigma,m} \psi_{a,s,l}^{\sigma,m}(r) Y_l^m(\theta, \phi) \xi_s^\sigma, \quad (13)$$

where  $\psi_{a,s,l}^{\sigma,m}(r)$  are radial wavefunctions,  $Y_l^m(\theta, \phi)$  are spherical harmonics, and  $\xi_s^\sigma$  are irreducible representations from the decomposition of the direct product of the spin states  $\chi_{J_{1,a}}^{M_{1,a}}$  and  $\chi_{J_{2,a}}^{M_{2,a}}$  of the particles 1 and 2,

$$\xi_s^\sigma = \sum_{M_{1,a}, M_{2,a}} \langle J_{1,a} J_{2,a} M_{1,a} M_{2,a} | J_{1,a} J_{2,a} s \sigma \rangle \chi_{J_{1,a}}^{M_{1,a}} \chi_{J_{2,a}}^{M_{2,a}}, \quad (14)$$

where the term with angle brackets is a Clebsch-Gordan coefficient. The sum over the total spin quantum number  $s$  ranges from  $|J_{1,a} - J_{2,a}|$  to  $J_{1,a} + J_{2,a}$ , and for each  $s$  the sum over the third component  $\sigma$  ranges from  $-s$  to  $+s$ . The sum over the orbital-angular-momentum quantum number  $l$  ranges from 0 to infinity, and for each  $l$  the sum over the third component  $m$  ranges from  $-l$  to  $+l$ . The radial wavefunctions in Equation (13) are labeled by quantum numbers  $\sigma$  and  $m$  for the third components of the spin and orbital angular momentum, respectively. It is more convenient to rewrite Equation (13) as an expansion in radial wavefunctions labeled by quantum numbers  $J$  and  $M$  for the total angular momentum,

$$\psi_a(\mathbf{r}) = \sum_{J,M} \sum_{s,l} \psi_{a,s,l}^{JM}(r) \sum_{\sigma,m} \langle sl\sigma m | slJM \rangle Y_l^m(\theta, \phi) \xi_s^\sigma. \quad (15)$$

The sum over  $J$  ranges from either 0 or  $\frac{1}{2}$  to infinity, and for each  $J$  the sum over the third component  $M$  ranges from  $-J$  to  $+J$ .

We derive the system of radial Schrödinger equations through the following steps:

1. Substitute Equation (15) into (12).
2. Multiply on the left by  $\sum_{\sigma', m'} \langle s'l'\sigma'm' | s'l'J'M' \rangle Y_{l'}^{m'}(\theta, \phi)^* \xi_{s'}^{\sigma'\dagger}$ .
3. Integrate over the angles  $\theta$  and  $\phi$ .
4. Impose conservation of angular momentum.

Once the above procedure has been applied to each channel  $a$ , one obtains infinitely many systems of radial Schrödinger equations labeled by conserved quantum numbers  $J$  and  $M$  for the total angular momentum and its third component. Using matrix notation, the system for given quantum numbers  $J$  and  $M$  can be written concisely as

$$\left[ \frac{1}{2\mu} \left( -\frac{d^2}{dr^2} - \frac{2}{r} \frac{d}{dr} + \frac{L(L+1)}{r^2} \right) + V^J(r) - E^J \right] \psi^{JM}(r) = 0, \quad (16)$$

where  $L$  is a diagonal orbital-angular-momentum matrix,  $V^J(r)$  is a radial potential matrix, and  $\psi^{JM}(r)$  is a vector wavefunction. Note that the wavefunctions depend on both  $J$  and  $M$ , but the potential and the energy depend only on  $J$ . The radial Schrödinger equations in this system are labeled by triplets  $(a, l, s)$  that identify spin-orbital channels of the scattering process. Since  $s$  and  $l$  are constrained by the triangle relations  $|J_{1,a} - J_{2,a}| \leq s \leq J_{1,a} + J_{2,a}$  and  $|J - s| \leq l \leq J + s$ , the system in Equation (16) contains only a finite number of radial Schrödinger equations for any value of  $J$ . To simplify the notation, we replace the labels  $(a, l, s)$  for the spin-orbital channels by a single integer  $i$ . Then the radial potential matrix elements can be expressed as

$$V_{ij}^J(r) = \sum_{\sigma_i, m_i} \sum_{\sigma_j, m_j} \langle s_i l_i \sigma_i m_i | s_i l_i J M \rangle \langle s_j l_j \sigma_j m_j | s_j l_j J M \rangle \times \int d\Omega Y_{l_i}^{m_i}(\theta, \phi)^* Y_{l_j}^{m_j}(\theta, \phi) \xi_{s_i}^{\sigma_i \dagger} V_{ab}(\mathbf{r}) \xi_{s_j}^{\sigma_j}, \quad (17)$$

where  $(a, s_i, l_i) \rightarrow i$ ,  $(b, s_j, l_j) \rightarrow j$ , and the total spin states  $\xi_{s_i}^{\sigma_i}$  and  $\xi_{s_j}^{\sigma_j}$  can be expanded in terms of the spin states  $\chi_{J_{1,i}}^{M_{1,i}}, \chi_{J_{2,i}}^{M_{2,i}}$  and  $\chi_{J_{1,j}}^{M_{1,j}}, \chi_{J_{2,j}}^{M_{2,j}}$  of particles 1, 2 in the channel  $i$  and  $j$  using Equation (14). Note that the right side of Equation (17) does not depend on  $M$  by virtue of the Wigner-Eckart theorem.

There is a somewhat common misunderstanding that the reduction of a three-dimensional Schrödinger equation to a radial form can be performed only for a spherically-symmetric potential that does not depend on the angles  $\theta$  and  $\phi$ . However, in our derivation of Equations (16) and (17) we have made no assumption on the potential  $V(\mathbf{r})$  other than it conserves angular momentum. In the trivial case where the potential is independent of spin, then conservation of angular momentum does indeed require that it is also spherically symmetric. If the potential does depend on spin, then it can also depend on the angles  $\theta$  and  $\phi$  but Equations (16) and (17) would still be valid. A brute-force method to determine if any given potential  $V(\mathbf{r})$  conserves angular momentum is to evaluate the right side of Equation (17) with  $J$  and  $M$  in one of the two Clebsch-Gordan coefficients replaced by  $J'$  and  $M'$ . The potential  $V(\mathbf{r})$  conserves angular momentum if and only if the result is zero for  $J' \neq J$  or  $M' \neq M$  and it is independent of  $M$  when  $J' = J$  and  $M' = M$ .

Equation (16) describes a scattering process taking place in a partial wave labeled by quantum numbers  $J$  and  $M$ . Because of conservation of angular momentum, each partial wave is decoupled from the others. SPARSE solves the scattering problem only for one individual partial wave, leaving the task of summing partial waves to the user. Hence, from now on we will drop all superscripts for the conserved quantum numbers  $J$  and  $M$ .

Finally, we can simplify the derivatives inside Equation (16) as follows. Let us observe that

$$\left( \frac{d^2}{dr^2} + \frac{2}{r} \frac{d}{dr} \right) \psi(r) = \frac{1}{r} \frac{d^2}{dr^2} u(r), \quad (18)$$

where we have introduced the reduced radial wavefunction

$$u(r) = r\psi(r). \quad (19)$$

Substituting Equation (18) into (16) and multiplying both sides by  $r$  yields

$$\left[ -\frac{1}{2\mu} \frac{d^2}{dr^2} + \frac{L(L+1)}{2\mu r^2} + V(r) - E \right] u(r) = 0. \quad (20)$$

Equation (20) is the system of radial Schrödinger equations solved by the SPARSE algorithm. It has  $N$  spin-orbital channels labeled by an integer  $i = 1, 2, \dots, N$ . The channel  $i$  has spin  $s_i$  and orbital angular momentum  $l_i$ . The reduced-mass matrix elements are  $\mu_{ij} = \delta_{ij}\mu_i$ . The orbital-angular-momentum matrix elements are  $L_{ij} = \delta_{ij}l_i$ . The radial potential matrix elements  $V_{ij}(r)$  are given in Equation (17).

### 3 Numerical solution

To solve Equation (20) numerically, we truncate and discretize the coordinate space for the distance  $r$  from  $\mathbb{R}_0^+$  to a finite grid of equally-spaced points  $\{r_n\}_{n=0}^{M+1}$ , where

$$r_n = nd \quad (21)$$

with  $d$  a small discretization step. Our discretized coordinate space begins at the origin  $r_0 = 0$ , has  $M$  points in its interior that we refer to as nodes, and ends at a finite but otherwise arbitrarily large radius  $r_{M+1} = R$ . The numerical reduced radial wavefunction in channel  $i$  is  $u_i(r_n)$ . The numerical potential matrix element between the channels  $i$  and  $j$  is  $V_{ij}(r_n)$ . The numerical second derivative of the reduced radial wavefunction is evaluated using the leading-order finite-difference method,

$$\frac{d^2}{dr^2} u(r_n) = \frac{u(r_{n-1}) - 2u(r_n) + u(r_{n+1}))}{d^2} + \mathcal{O}(d^4). \quad (22)$$

For small enough discretization steps  $d$ , the  $\mathcal{O}(d^4)$  corrections can be neglected.

To close the system of equations, we fix the values of the reduced radial wavefunctions at the boundaries,  $u_i(0)$  and  $u_i(R)$ . This is referred to as imposing Dirichlet boundary conditions. We can choose the physical boundary conditions using the known analytical behavior of the solutions to Equations

tion (20) for  $r \rightarrow 0$  and  $r \rightarrow \infty$ . Since a physical solution  $u_i(r)$  goes to zero as  $r^{l_i+1}$  for  $r \rightarrow 0$ , we impose

$$u_i(0) = 0. \quad (23)$$

The boundary condition at large  $r$  is more complicated. For physical scattering problems, one has

$$\lim_{r \rightarrow \infty} V_{ij}(r) = \delta_{ij} V_i^\infty \quad (24)$$

where each  $V_i^\infty$  is either a definite number or positive infinity. We identify  $V_i^\infty$  with the energy threshold where the scattering channel  $i$  opens up. The boundary condition for  $u_i(R)$  depends on whether the energy  $E$  in the Schrödinger equation is larger or smaller than the threshold  $V_i^\infty$ . If  $E < V_i^\infty$ , then a physical solution goes to zero for  $r \rightarrow \infty$  and we impose  $u_i(R) = 0$ . If otherwise  $E > V_i^\infty$ , a physical solution keeps oscillating indefinitely for  $r \rightarrow \infty$ . It is however a specific, finite number at the maximum distance  $R$  in our truncated coordinate space. So, we impose  $u_i(R) = b_i$ , where  $b_i$  is a real constant. We can conveniently impose the boundary condition for both cases  $E < V_i^\infty$  and  $E \geq V_i^\infty$  at once in the form

$$u_i(R) = \theta(E - V_i^\infty) b_i, \quad (25)$$

where

$$\theta(x) = \begin{cases} 0 & \text{if } x < 0, \\ 1 & \text{if } x \geq 0, \end{cases} \quad (26)$$

is the Heaviside step function.

Using Equations (22), (23), and (25), we reduce Equation (20) down to a system of numerical Schrödinger equations,

$$\sum_{j,m} [H_{ij,nm} - \delta_{ij} \delta_{nm} E] u_j(r_m) = \delta_{nM} \theta(E - V_i^\infty) \frac{b_i}{2\mu_i d^2}, \quad (27)$$

where  $H_{ij, nm}$  are the numerical Hamiltonian matrix elements

$$H_{ij, nm} = -\delta_{ij} \frac{\delta_{(n-1)m} - 2\delta_{nm} + \delta_{(n+1)m}}{2\mu_i d^2} + \delta_{ij} \delta_{nm} \frac{l_i(l_i + 1)}{2\mu_i r_n^2} + \delta_{nm} V_{ij}(r_n) \quad (28)$$

with  $i, j = 1, \dots, N$  denoting channels and  $n, m = 1, \dots, M$  denoting nodes. The numerical Hamiltonian is a matrix with  $N^2 M^2$  elements, but only a small fraction of them are different from zero. The ratio of nonzero elements over the total scales like  $1/M$ , with  $M$  being a very large number for a large maximum distance  $R$  and a small discretization step  $d$ . The numerical Hamiltonian in Equation (28) is therefore a sparse matrix.

To input the Schrödinger equation into SPARSE, the user has to provide the following information:

- The orbital angular momentum  $l_i$ , reduced mass  $\mu_i$ , and threshold  $V_i^\infty$  for each channel  $i$ .
- The positions of the nodes  $r_n$  and the numerical potential matrix elements  $V_{ij}(r_n)$ .

SPARSE reads this information from two comma-separated-values (CSV) files named `channels.csv` and `potential.csv`, which must be placed within the working directory.

The file `channels.csv` must have one line for the header followed by  $N$  lines for the values. Each line must contain at least three entries. The header must contain at least the following strings: `l`, `mu`, and `threshold`. The following  $N$  lines must contain at least the corresponding values for the channels  $i = 1, \dots, N$ . An entry under `l` is an integer indicating  $l_i$ . An entry under `mu` is a decimal number indicating  $\mu_i$ . An entry under `threshold` is a decimal number indicating  $V_i^\infty$  or `inf` if  $V_i^\infty = \infty$ . The ordering of the columns is irrelevant, but it must obviously be consistent between rows. Below is the typical structure of a minimal `channels.csv` file.

```
l,mu,threshold
l1,mu1,T1
l2,mu2,T2
```

...  
 1N,muN,TN

For the user's convenience, additional information about the channels may be specified by adding more columns to the file `channels.csv`. For instance, the user may want to include a column named `s` indicating the spin  $s_i$  for each channel  $i$ , or a column named `channel` providing a label for each channel that is more informative than just the integer  $i$ . Such additional columns will be read by SPARSE but will not play any role in the calculation.

The file `potential.csv` must have no header and  $M$  lines for the values. Each line must contain exactly  $N^2 + 1$  entries. The first entry is the node position  $r_n$ . The following  $N^2$  entries are the numerical values of the flattened potential matrix,  $V_{ij}(r_n)$ . SPARSE assumes that the potential matrix is flattened in row-major (C-style) order.<sup>2</sup> Below is the typical structure of the `potential.csv` file.

```
r1,V11(r1),V12(r1),...,VNN(r1)
r2,V11(r1),V12(r2),...,VNN(r2)
...
rM,V11(rM),V12(rM),...,VNN(rM)
```

SPARSE reads the values from the two CSV files and stores them into two pandas `DataFrame` objects using the function `read_csv` from the pandas library [7]. From them, SPARSE calculates the Hamiltonian matrix elements  $H_{ij,nm}$  from Equation (28) and writes them into a 2-dimensional NumPy `array` object [8] with elements  $H_{\mu\nu}$ . This reshaping amounts to applying an invertible map  $(i, n) \mapsto \mu$  from pairs of indices  $i = 1, \dots, N$  and  $n = 1, \dots, M$  to a single index  $\mu = 1, \dots, NM$ . SPARSE reads the matrix elements from Equation (28) and writes them in the NumPy `array` following a C-style index order, which corresponds to setting

$$\mu = i + N(n - 1). \quad (29)$$

This choice of index order has the advantage that all the nonzero  $H_{\mu\nu}$  end up

---

<sup>2</sup>This fact is irrelevant if the potential is a symmetric matrix.

as close as possible to the main diagonal. From Equation (28), we see that the only nonzero  $H_{ij, nm}$  are those with  $i = j$  and  $|n - m| \leq 1$  or those with  $n = m$  and  $|i - j| \leq N - 1$ . Then it follows from Equation (29) that the only nonzero  $H_{\mu\nu}$  are those with

$$|\mu - \nu| \leq |i - j| + N|n - m| \leq N. \quad (30)$$

Therefore the  $H_{\mu\nu}$  form the elements of a banded matrix where all the nonzero elements are contained within the main diagonal, the first  $N$  upper diagonals, and the first  $N$  lower diagonals.

SPARSE writes the Hamiltonian in the matrix diagonal ordered form, which is a 2-dimensional array consisting of only the  $2N + 1$  nonzero diagonals stacked from top to bottom. The upper and lower diagonals are padded so that they all have the same number of elements  $NM$  as the main diagonal. The matrix diagonal ordered form has only  $(2N + 1) \times (NM)$  elements, and therefore it occupies significantly less memory than the full  $(NM) \times (NM)$  numerical Hamiltonian matrix with its many zeroes. Consider for example a system with  $N = 4$  channels and  $M = 10^6$  nodes using 64-bit floating-point numbers. The matrix diagonal ordered form would take 288 megabytes of memory, as opposed to a staggering 128 terabytes for the full matrix! If not for this memory optimization, it would be all but impossible to accurately solve a large system of Schrödinger equations using the finite-difference method.

We therefore redefine the indices of Equation (27) as  $(i, n) \rightarrow \mu$  and  $(j, m) \rightarrow \nu$  using Equation (29), which reshapes Equation (27) into an ordinary nonhomogeneous linear system,

$$\sum_{\nu} (H_{\mu\nu} - \delta_{\mu\nu} E) u_{\nu} = B_{\mu}(E), \quad (31)$$

where the constant vector is

$$B_{\mu}(E) = \delta_{nM} \theta(E - V_i^{\infty}) \frac{b_i}{2\mu_i d^2}. \quad (32)$$

Note that if  $E < V_i^{\infty}$  for all  $i$ , which corresponds to a bound state, then

$B_\mu(E) = 0$  for all  $\mu$  and Equation (31) becomes an eigenvalue problem for the Hamiltonian matrix. Even though SPARSE is primarily designed for calculating scattering states, it also contains a handy bound-state calculator which solves Equation (31) with  $B_\mu(E) = 0$  using the function `eigsh` from the sparse linear algebra module of SciPy [9].

Finally, a note about measuring units. SPARSE uses natural units, in which  $\hbar = c = 1$  and therefore  $[\text{Time}] = [\text{Length}]$ ,  $[\text{Mass}] = [\text{Energy}]$ , and  $[\text{Length}] = [\text{Energy}]^{-1}$ . There is only one independent dimension, typically chosen between  $[\text{Length}]$  in units of fm (femtometers) and  $[\text{Energy}]$  in units of eV (electron Volts). The conversion between length-based and energy-based units is easily achieved by means of the formula  $\hbar c = 1 = 197.327 \text{ MeV fm}$ . The SPARSE algorithm is agnostic to the user's choice of units, but it assumes that the dimension of the inputs are  $[r_n] = [\text{Length}]$  and  $[V_{ij}(r_n)] = [\mu_i] = [V_i^\infty] = [\text{Energy}]$ .

## 4 Calculating the $K$ -matrix

From now on we shall assume, without loss of generality, that the channels  $i$  are ordered in increasing threshold value. It is worth noting that the SPARSE algorithm does not require the input channels to be sorted in any particular way. The assumption  $V_i^\infty \geq V_j^\infty$  for any  $i \geq j$  is only made to simplify the notation in this paper.

For a given energy  $E$ , the possible values of the constant in Equation (32) constitute a vector space of dimension  $O$ , where  $O$  is the number of open channels  $i$  whose threshold is less than  $E$ ,  $V_i^\infty \leq E$  for  $i = 1, \dots, O$ . We can easily construct a basis for this vector space by substituting  $b_i$  inside Equation (32) with

$$b_{ij} = \delta_{ij}, \quad (33)$$

where the first index  $i = 1, \dots, N$  labels the channels and the second index  $j = 1, \dots, O$  labels the vectors in the basis. Plugging Equation (33) into (32), we obtain a constant term with two indices,  $B_{\mu j}(E)$ , which we can treat as the elements of a  $(NM) \times O$  matrix  $B$ , dropping its dependence on  $E$ . We

also define the  $(NM) \times (NM)$  matrix

$$A = H - EI. \quad (34)$$

with  $I$  the identity matrix.  $A$  is a banded matrix which SPARSE calculates by shifting the main diagonal of the numerical Hamiltonian by  $-E$  in the matrix diagonal ordered form. With these definitions, we rewrite Equation (31) as a matrix equation

$$Au = B, \quad (35)$$

where  $u$  is a  $(NM) \times O$  matrix whose columns are the linearly independent solutions to Equation (31) with the same energy  $E$ .

For any energy  $E$ , SPARSE constructs the matrices  $A$  and  $B$  using Equations (32)-(34) and solves Equation (35) for the matrix  $u$  using the function `solve_banded` from the linear algebra module of SciPy [9]. Then, SPARSE reshapes the matrix  $u$  into a set of numerical reduced wavefunctions using Equation (29):  $\mu \rightarrow (i, n)$ ,  $u_{\mu j} \rightarrow u_{ij}(r_n)$ . Next, we use these numerical wavefunctions to calculate the reactance matrix  $K$  for the scattering process. We will disregard from now on wavefunction components for confining channels  $i$  with  $V_i^\infty = \infty$ , which are irrelevant to the scattering states at large  $r$ .

First, we define the numerical range of the potential  $r_V$  as the maximum value of  $r$  for which any potential matrix element<sup>3</sup> is significantly different from its limiting value at  $r \rightarrow \infty$ ,

$$r_V = \max \left\{ r \mid \left\| V(r) - \lim_{r \rightarrow \infty} V(r) \right\| > \epsilon \right\}, \quad (36)$$

where  $\epsilon$  is a fixed small number.

Next, we review the analytic wavefunctions of the scattering states at large  $r$ . For  $r \gg r_V$ , Equation (20) reduces to a set of decoupled Schrödinger equations for free particles,

$$\left[ -\frac{1}{2\mu_i} \frac{d^2}{dr^2} + \frac{l_i(l_i + 1)}{2\mu_i r^2} + V_i^\infty - E \right] u_i(r) = 0, \quad (37)$$

---

<sup>3</sup>Excluding diagonal elements for confining channels.

for every channel  $i$  with a finite threshold  $V_i^\infty$ . For a closed channel  $i$  with  $V_i^\infty > E$  ( $i = O + 1, \dots, N$ ), a physical solution to Equation (37) must approach zero at large distances. For an open channel  $i$  with  $V_i^\infty \leq E$  ( $i = 1, \dots, O$ ), Equation (37) has two linearly independent physical solutions. Using real boundary conditions and wavefunction normalization by energy (see Reference [10] for alternative conventions), the two solutions are

$$\sqrt{\frac{2\mu_i}{\pi p_i}} S_{l_i}(p_i r) \quad \text{and} \quad \sqrt{\frac{2\mu_i}{\pi p_i}} C_{l_i}(p_i r), \quad (38)$$

where  $p_i$  is the scattering momentum in the open channel  $i$ ,

$$p_i = \sqrt{2\mu_i(E - V_i^\infty)}, \quad (39)$$

and  $S_l(x)$  and  $C_l(x)$  are the Riccati-Bessel functions

$$S_l(x) = x j_l(x), \quad (40)$$

$$C_l(x) = -x y_l(x), \quad (41)$$

with  $j_l(x)$  and  $y_l(x)$  the spherical Bessel functions of the first and second kind, respectively. The asymptotic solution of any Schrödinger equation that coincides with Equation (37) at large  $r$  can be written as a linear combination of the solutions in Equation (38). In particular, the asymptotic wavefunctions for a complete set of scattering states with energy  $E$  can be expressed as

$$u_{ij}(r) \simeq \sqrt{\frac{2\mu_i}{\pi p_i}} (S_{l_i}(p_i r) + K_{ij} C_{l_i}(p_i r)), \quad (42)$$

where the relation “ $\simeq$ ” stands for equality at large  $r$ , the first index  $i = 1, \dots, O$  labels open channels, the second index  $j = 1, \dots, O$  labels linearly independent solutions with the same energy, and  $K_{ij}$  are  $K$ -matrix elements (see Section 11.1.2 of Reference [11]).

Next, we compare the numerical wavefunctions  $u_{ij}(r_n)$  to the analytic asymptotic wavefunctions in Equation (42) to extract the  $K$ -matrix elements. The numerical wavefunctions calculated from Equation (35) generally do not

correspond to the asymptotic scattering states in Equation (42). Instead, the numerical wavefunctions at large  $r$  correspond to a more general linear combination of Riccati-Bessel functions,

$$u_{ij}(r) \simeq \sqrt{\frac{2\mu_i}{\pi p_i}} (X_{ij} S_{l_i}(p_i r) + Y_{ij} C_{l_i}(p_i r)), \quad (43)$$

where  $X_{ij}$  and  $Y_{ij}$  are real constants that can be regarded as the elements of two matrices  $X$  and  $Y$ . Comparing Equations (42) and (43), we see that the  $K$ -matrix can be calculated from the matrices  $X$  and  $Y$  using

$$K = Y X^{-1}. \quad (44)$$

The matrices  $X$  and  $Y$  depend on the choice of the matrix constant  $B$  in Equation (35), but the  $K$ -matrix does not. If instead of  $B$  we had chosen any other admissible  $B'$ , then instead of  $X$  and  $Y$  we would have obtained  $X' = XW$  and  $Y' = YW$  with  $W = B^{-1}B'$  an invertible  $O \times O$  matrix. However, the  $K$ -matrix from Equation (44) would have been the same.

Finally, let us show how to calculate the matrices  $X$  and  $Y$  explicitly from the numerical wavefunctions  $u_{ij}(r_n)$ . Consider the asymptotic wavefunction in Equation (43) and take the further limit  $r \gg l_i/p_i$ , which yields

$$u_{ij}(r) \simeq \sqrt{\frac{2\mu_i}{\pi p_i}} \left( X_{ij} \sin\left(p_i r - l_i \frac{\pi}{2}\right) + Y_{ij} \cos\left(p_i r - l_i \frac{\pi}{2}\right) \right). \quad (45)$$

Now consider the following system of equations

$$\begin{cases} \mathcal{S}_{ij} = \sqrt{\frac{2\pi p_i^3}{\mu_i}} \int_{\rho_i}^R u_{ij}(r) \sin\left(p_i r - l_i \frac{\pi}{2}\right) dr \\ \mathcal{C}_{ij} = \sqrt{\frac{2\pi p_i^3}{\mu_i}} \int_{\rho_i}^R u_{ij}(r) \cos\left(p_i r - l_i \frac{\pi}{2}\right) dr \end{cases}, \quad (46)$$

where the upper integration limit is the maximum radius  $R$  and the lower integration limit  $\rho_i$  satisfies

$$\rho_i \gg r_V \quad \text{and} \quad \rho_i \gg l_i/p_i, \quad (47)$$

with  $r_V$  the potential radius. The integrals  $\mathcal{S}_{ij}$  and  $\mathcal{C}_{ij}$  in Equation (46) are obviously convergent since the wavefunctions  $u_{ij}(r)$  are linear combinations of sine and cosine functions in the integration interval. In fact, the integrals  $\mathcal{S}_{ij}$  and  $\mathcal{C}_{ij}$  can be expressed analytically in terms of  $X_{ij}$  and  $Y_{ij}$  by inserting Equation (45) and integrating the products of sine and cosine functions using

$$\int_{x_0}^{x_1} \sin^2(x) dx = \frac{x_1 - x_0}{2} - \frac{1}{4}(\sin(2x_1) - \sin(2x_0)), \quad (48a)$$

$$\int_{x_0}^{x_1} \cos^2(x) dx = \frac{x_1 - x_0}{2} + \frac{1}{4}(\sin(2x_1) - \sin(2x_0)), \quad (48b)$$

$$\int_{x_0}^{x_1} \sin(x) \cos(x) dx = -\frac{1}{4}(\cos(2x_1) - \cos(2x_0)). \quad (48c)$$

Thus Equation (46) becomes

$$\begin{cases} \mathcal{S}_{ij} = (\alpha_i - \beta_i)X_{ij} - \gamma_i Y_{ij} \\ \mathcal{C}_{ij} = -\gamma_i X_{ij} + (\alpha_i + \beta_i)Y_{ij} \end{cases}, \quad (49)$$

where we have introduced the shorthand

$$\alpha_i = R - \rho_i, \quad (50a)$$

$$\beta_i = \frac{1}{2}(\sin(2R) - \sin(2\rho_i)), \quad (50b)$$

$$\gamma_i = \frac{1}{2}(\cos(2R) - \cos(2\rho_i)). \quad (50c)$$

The linear system in Equation (49) can be inverted to express  $X_{ij}$  and  $Y_{ij}$  in terms of the integrals  $\mathcal{S}_{ij}$  and  $\mathcal{C}_{ij}$ ,

$$\begin{cases} X_{ij} = \frac{1}{\alpha_i^2 - \beta_i^2 - \gamma_i^2} [(\alpha_i + \beta_i)\mathcal{S}_{ij} + \gamma_i\mathcal{C}_{ij}] \\ Y_{ij} = \frac{1}{\alpha_i^2 - \beta_i^2 - \gamma_i^2} [\gamma_i\mathcal{S}_{ij} + (\alpha_i - \beta_i)\mathcal{C}_{ij}] \end{cases}. \quad (51)$$

Therefore, we can obtain the numerical values of  $X_{ij}$  and  $Y_{ij}$  by evaluating the integrals  $\mathcal{S}_{ij}$  and  $\mathcal{C}_{ij}$  in Equation (46) using the numerical wavefunctions

$u_{ij}(r_n)$  and Simpson's rule. SPARSE uses the `simpson` function from the integration module of SciPy [9]. As long as the momenta  $p_i$  satisfy  $p_i \ll d^{-1}$ , the integrands of  $\mathcal{S}_{ij}$  and  $\mathcal{C}_{ij}$  are slowly oscillating functions with respect to the discretization step  $d$ . Then Simpson's rule provides an accurate numerical estimate of the integrals  $\mathcal{S}_{ij}$  and  $\mathcal{C}_{ij}$  in Equation (46).

## 5 Scattering poles and amplitudes

We define the transition matrix  $T$  in terms of the scattering matrix  $S$  as

$$S = I + 2iT. \quad (52)$$

Within this convention, a  $T$ -matrix element  $T_{ij}$  corresponds to the partial-wave scattering amplitude  $f_{i \leftarrow j}$  from an initial channel  $j$  to a final channel  $i$  times the relative momentum in the final channel,

$$T_{ij} = p_i f_{i \leftarrow j}. \quad (53)$$

Scattering resonances are associated with poles of the scattering amplitude for energies in the lower half of the complex plane.

The reactance matrix  $K$  is defined as the Cayley transform of the  $S$ -matrix,

$$K = i \frac{I - S}{I + S}, \quad (54)$$

which can be inverted to give

$$S = \frac{I + iK}{I - iK} \quad (55)$$

(see Section 14-e of Reference [12]). We see from Equations (54) and (55) that unitarity ( $S^\dagger = S^{-1}$ ) and time-reversal symmetry ( $S^\top = S$ ) require that the  $K$ -matrix is real and symmetric. The  $K$ -matrix calculated using Equations (44), (46), and (51) is real by definition. It is only approximately symmetric within numerical errors. Let us call this approximately symmetric

matrix  $\tilde{K}$ . SPARSE calculates the degree of asymmetry as

$$\max_{ij} \left\{ \frac{|\tilde{K}_{ij} - \tilde{K}_{ji}|}{|\tilde{K}_{ij} + \tilde{K}_{ji}|} \right\} \quad (56)$$

and warns the user if it is larger than a tolerance (1% by default). Then SPARSE calculates the exactly symmetric  $K$ -matrix as

$$K = \frac{\tilde{K} + \tilde{K}^\top}{2}. \quad (57)$$

Resonances may appear as poles of the  $K$ -matrix on the real axis of the physical Riemann sheet. For energies near the pole, the  $K$ -matrix elements can be expressed as

$$K_{ij} = g_i g_j \frac{\Gamma/2}{M - E} + K_{ij}^{\text{nonres}}. \quad (58)$$

where  $K_{ij}^{\text{nonres}}$  is a “nonresonant” contribution that is regular at the pole energy<sup>4</sup> and  $M$ ,  $\Gamma$ , and  $g_i$  are respectively the mass of the resonance, its width, and its coupling to the channel  $i$ . The couplings  $g_i$  are normalized,  $\sum_i g_i^2 = 1$ , so that the couplings squared give the branching ratios of the resonance,

$$B_i = g_i^2. \quad (59)$$

SPARSE calculates scattering poles by interpolating between numerical  $K$ -matrix elements obtained at a set of discrete energies. The interpolation is performed using the AAA algorithm for rational polynomial approximation [13], which yields the pole energies  $M$  and the residues of the  $K$ -matrix elements at the poles,

$$R_{ij} = \text{Res}_M(K_{ij}). \quad (60)$$

Not all poles of the  $K$ -matrix correspond to resonances. SPARSE identifies  $K$ -matrix poles associated to resonances by comparing the residues calculated from the AAA algorithm with the analytic pole term in Equation (58). If the  $K$ -matrix pole indeed corresponds to a resonance, then Equations (58) and

---

<sup>4</sup>Contributions from other poles at different energies may be contained in this term.

(60) require

$$R_{ij} = -g_i g_j \Gamma / 2, \quad (61)$$

which implies two constraints on the residues:

$$R_{ii} < 0 \quad \text{and} \quad R_{ij}^2 = R_{ii} R_{jj} \quad (62)$$

for every  $i$  and  $j$ . SPARSE calculates the residues  $R_{ij}$  and checks that they satisfy the constraints in Equation (62). If the constraints are satisfied, SPARSE calculates the width of the resonance as

$$\Gamma = -2 \sum_i R_{ii}, \quad (63)$$

then it calculates the couplings as

$$g_i = \text{sgn}(-R_{1i}) \sqrt{-2R_{ii}/\Gamma}, \quad (64)$$

where the sign function on the right side is necessary to fix the relative signs between the couplings so that they agree with Equation (61). Note that the couplings are defined up to an overall sign, that is, the  $K$ -matrix in Equation (58) is invariant if we substitute  $g_i \rightarrow -g_i$  for every  $i$ . In writing Equation (64), we have chosen the convention  $g_i \geq 0$  for  $i = 1$ .

The scattering amplitudes  $f_{i \leftarrow j}$  can be calculated from the numerical  $K$ -matrix elements by inserting Equation (55) into (52), which gives

$$T = \frac{K}{I - iK}, \quad (65)$$

and using Equation (53). The corresponding partial-wave cross-section,  $\sigma_{i \leftarrow j}$ , is proportional to the square modulus of the scattering amplitudes,

$$\sigma_{i \leftarrow j} = \frac{4\pi(2J+1)}{(2J_{1,j}+1)(2J_{2,j}+1)} |f_{i \leftarrow j}|^2, \quad (66)$$

where  $J$  is the total angular momentum and  $J_{1,j}$  and  $J_{2,j}$  are the spins of the particles 1 and 2 in the initial channel  $j$ . The total unpolarized cross

Table 1: Integer label  $i$ , orbital angular momentum  $l$ , reduced mass  $\mu$ , and threshold  $V^\infty$  for the channels in the SPARSE showcase example. Units are arbitrary.

$i$	$l$	$\mu$	$V^\infty$
1	1	1000	0
2	0	1000	100

section can be obtained by summing over the spins  $s_i, s_j$ , the orbital angular momenta  $l_i, l_j$ , and the total angular momentum  $J$ .

It is worth noting that the mass  $M$ , width  $\Gamma$ , and couplings  $g_i$  obtained from the  $K$ -matrix pole are generally not the same as the parameters of the *bona fide* resonance, that is, the  $T$ -matrix pole. However, the parameters of the  $K$ -matrix and  $T$ -matrix poles do coincide in the case of an isolated resonance. To see this, insert Equation (58) into Equation (65) keeping only the pole term and observe that the result is the resonant  $T$ -matrix element:

$$T_{ij} \approx ig_i g_j \frac{i\Gamma/2}{E - M + i\Gamma/2}. \quad (67)$$

If the resonance is not isolated, then the parameters  $M$ ,  $\Gamma$ , and  $g_i$  obtained from the  $K$ -matrix pole can differ significantly from those of the  $T$ -matrix pole. Nonetheless, the  $K$ -matrix pole parameters are physically relevant as they can be related to  $K$ -matrix fits to experimental data. In those cases where a distinction is necessary,  $M$ ,  $\Gamma$ , and  $g_i$  may be referred to as the *nominal* mass, width, and couplings of the resonance.

## 6 Showcase

Next, we examine an application of the SPARSE algorithm to a relatively simple system with two coupled channels. Units are arbitrary. The two channels are described in Table 1. The potential matrix is

$$V(r) = \begin{pmatrix} V_{11}(r) & V_{12}(r) \\ V_{21}(r) & V_{22}(r) \end{pmatrix}. \quad (68)$$

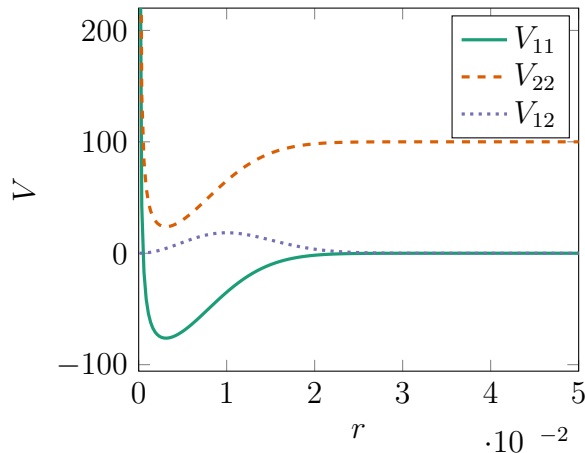


Figure 1: Potential matrix elements for the SPARSE showcase example. Axes have arbitrary units.

The first diagonal element  $V_{11}(r)$  is a potential well with a short-distance repulsion,

$$V_{11}(r) = \left( \frac{0.05}{r} - 100 \right) \exp(-(100r)^2). \quad (69)$$

The second diagonal element  $V_{22}(r)$  is the same potential well but shifted by +100,

$$V_{22}(r) = V_{11}(r) + 100. \quad (70)$$

The offdiagonal element  $V_{12}(r) = V_{21}(r)$  is Gaussian coupling potential,

$$V_{12}(r) = 50(100r)^2 \exp(-(100r)^2). \quad (71)$$

The coordinate space of  $r$  is a grid of points in the interval  $[0, 1]$  with a discretization step  $d = 10^{-6}$ . The potential  $V_{11}(r)$  has been engineered so that it has a  $P$ -wave (that is,  $l = 1$ ) bound state with energy somewhat below the first threshold,  $V_1^\infty = 0$ . The potential  $V_{22}(r)$  has been engineered so that in isolation it would have an  $S$ -wave (that is,  $l = 0$ ) bound state with energy somewhat below the second threshold,  $V_2^\infty = 100$ . The coupling potential  $V_{12}(r)$  has been engineered so that the would-be bound state in the second channel appears instead as a narrow scattering resonance in the first channel. These potential matrix elements are plotted in Figure 1.

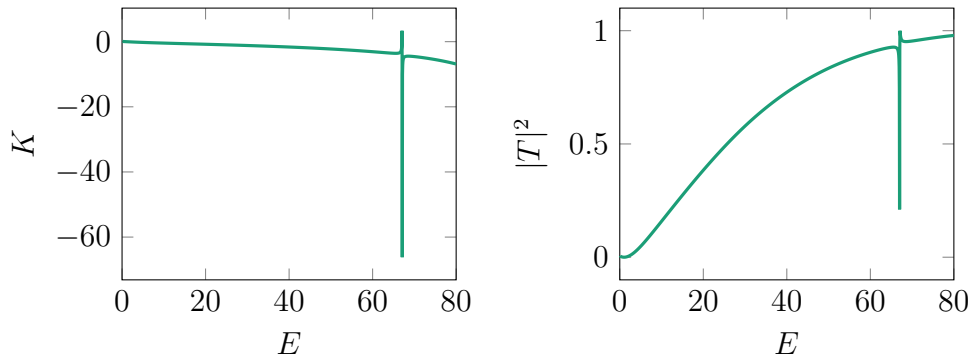


Figure 2:  $K$ -matrix (left) and square modulus of the  $T$ -matrix (right) in the SPARSE showcase example. The horizontal axes have arbitrary units.

We use SPARSE to calculate the  $K$ -matrix for a grid of energies in the interval  $[0, 80]$  with a constant spacing of 0.05. The  $K$ -matrix has only one element, since there is only one open channel in this energy region. We plot the  $K$ -matrix as a function of the energy in the left panel of Figure 2. We also calculate the square modulus of the  $T$ -matrix element and plot it in the right panel of Figure 2.

The scattering amplitude looks complicated because it results from the overlap of two different line shapes. The smooth enhancement is due to the bound state in channel 1, which has an energy of -12.5. The sharp oscillation of the amplitude in between 60 and 80 is due to a resonance. That oscillation in  $|T|^2$  matches a pole of the  $K$ -matrix with mass  $M = 67.09$  and width  $\Gamma = 0.66$ .

The SPARSE repository contains a Python script that prepares the CSV files `channels.csv` and `potential.csv` used for this example. It also contains a handy IPython notebook which reproduces the results of this section using the SPARSE Application Programming Interface. The reader is invited to go through the IPython notebook as a tutorial for using SPARSE.

## 7 Summary

SPARSE is a simple and efficient Python algorithm for the calculation of amplitudes and resonances for inelastic scattering in nonrelativistic quantum

mechanics. SPARSE solves a system of coupled radial Schrödinger equations that represents a partial wave of a two-body scattering process in systems where the particles can change their state as a result of the collision. The SPARSE algorithm is optimized for the application to systems with tens of coupled Schrödinger equations. It reduces the system of differential equations to a nonhomogeneous linear system by approximating the second derivative using the finite-difference method and imposing Dirichlet boundary conditions. It calculates the numerical wavefunctions by solving the system, then compares them to the analytical wavefunctions of scattering states to obtain the  $K$ -matrix elements. Finally, SPARSE calculates scattering amplitudes and poles from the  $K$ -matrix elements for real energies.

The only inputs required by SPARSE are the orbital angular momenta, reduced masses, and thresholds for the each of the Schrödinger equations in the system plus the numerical coordinate space and potential matrix. These numerical inputs are provided by the user in the form of two CSV files named `channels.csv` and `potential.csv`. The user can calculate these numerical inputs using any computational software. The SPARSE Application Programming Interface is designed so that it can be used with minimal Python literacy. The SPARSE repository also contains a Python script that creates working examples for the input CSV files. It also contains an IPython notebook which showcases the program's functionality and serves as a useful tutorial.

## Acknowledgements

This work was supported in part by the U.S. Department of Energy under grant DE-SC0011726. I would like to thank F. Alasiri for beta testing the program. I would also like to thank A. Rodas for discussions during the HADRON 2025 conference.

## References

- [1] V. N. Kaliakin, *Introduction to Approximate Solution Techniques, Numerical Modeling, and Finite Element Methods* (Marcel Dekker, New York, 2002).
- [2] D. E. Manolopoulos, “An improved log derivative method for inelastic scattering”, [The Journal of Chemical Physics](#) **85**, 6425 (1986).
- [3] J. C. Butcher, “A history of runge-kutta methods”, *Applied numerical mathematics* **20**, 247 (1996).
- [4] S. A. Orszag, “Spectral methods for problems in complex geometries”, [Journal of Computational Physics](#) **37**, 70 (1980).
- [5] J. Lill, G. Parker, and J. Light, “Discrete variable representations and sudden models in quantum scattering theory”, [Chemical Physics Letters](#) **89**, 483 (1982).
- [6] R. Bruschini and P. González, “Coupled-channel meson-meson scattering in the diabatic framework”, [Phys. Rev. D](#) **104**, 074025 (2021), [arXiv:2107.05459 \[hep-ph\]](#).
- [7] W. McKinney, “Data Structures for Statistical Computing in Python”, in [Proceedings of the 9th Python in Science Conference](#) (2010), pp. 56–61.
- [8] C. R. Harris, K. J. Millman, S. J. van der Walt, R. Gommers, P. Virtanen, D. Cournapeau, E. Wieser, J. Taylor, S. Berg, N. J. Smith, R. Kern, M. Picus, S. Hoyer, M. H. van Kerkwijk, M. Brett, A. Haldane, J. F. del Río, M. Wiebe, P. Peterson, P. Gérard-Marchant, K. Sheppard, T. Reddy, W. Weckesser, H. Abbasi, C. Gohlke, and T. E. Oliphant, “Array programming with NumPy”, [Nature](#) **585**, 357 (2020).
- [9] P. Virtanen, R. Gommers, T. E. Oliphant, M. Haberland, T. Reddy, D. Cournapeau, E. Burovski, P. Peterson, W. Weckesser, J. Bright, S. J. van der Walt, M. Brett, J. Wilson, K. J. Millman, N. Mayorov, A. R. J. Nelson, E. Jones, R. Kern, E. Larson, C. J. Carey, Í. Polat, Y. Feng, E. W. Moore, J. VanderPlas, D. Laxalde, J. Perktold, R. Cimrman, I. Henriksen, E. A. Quintero, C. R. Harris, A. M. Archibald, A. H. Ribeiro,

- F. Pedregosa, P. van Mulbregt, and SciPy 1.0 Contributors, “SciPy 1.0: Fundamental Algorithms for Scientific Computing in Python”, [Nature Methods](#) **17**, 261 (2020).
- [10] M. A. Morrison and A. N. Feldt, “Through scattering theory with gun and camera: coping with conventions in collision theory”, [American Journal of Physics](#) **75**, 67 (2007).
- [11] R. G. Newton, *Scattering Theory of Waves and Particles* (Springer Berlin, Heidelberg, 2013).
- [12] J. R. Taylor, *Scattering Theory: The Quantum Theory of Nonrelativistic Collisions* (Robert E. Krieger, Malabar, 1983).
- [13] Y. Nakatsukasa, O. Sète, and L. N. Trefethen, “The AAA Algorithm for Rational Approximation”, [SIAM Journal on Scientific Computing](#) **40**, A1494 (2018).